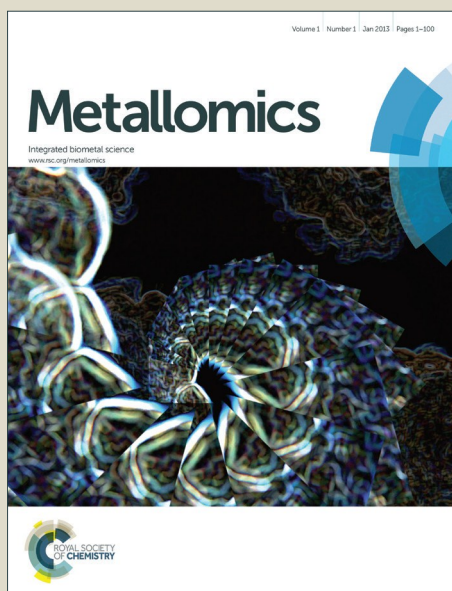


Metallomics

Accepted Manuscript



This is an *Accepted Manuscript*, which has been through the Royal Society of Chemistry peer review process and has been accepted for publication.

Accepted Manuscripts are published online shortly after acceptance, before technical editing, formatting and proof reading. Using this free service, authors can make their results available to the community, in citable form, before we publish the edited article. We will replace this *Accepted Manuscript* with the edited and formatted *Advance Article* as soon as it is available.

You can find more information about *Accepted Manuscripts* in the [Information for Authors](#).

Please note that technical editing may introduce minor changes to the text and/or graphics, which may alter content. The journal's standard [Terms & Conditions](#) and the [Ethical guidelines](#) still apply. In no event shall the Royal Society of Chemistry be held responsible for any errors or omissions in this *Accepted Manuscript* or any consequences arising from the use of any information it contains.

ARTICLE

Loss of *pdr-1/parkin* influences Mn homeostasis through altered *ferroportin* expression in *C. elegans*

Cite this: DOI: 10.1039/x0xx00000x

Sudipta Chakraborty^a, Pan Chen^b, Julia Bornhorst^c, Tanja Schwerdtle^c, Fabian Schumacher^{c,d}, Burkhard Kleuser^c, Aaron B. Bowman^e and Michael Aschner^b

Received 00th November 2013,
Accepted

DOI: 10.1039/x0xx00000x

www.rsc.org/

Overexposure to the essential metal manganese (Mn) can result in an irreversible condition known as manganism that shares similar pathophysiology with Parkinson's disease (PD), including dopaminergic (DAergic) cell loss that leads to motor and cognitive impairments. However, the mechanisms behind this neurotoxicity and its relationship with PD remain unclear. Many genes confer risk for autosomal recessive, early-onset PD, including the *parkin/PARK2* gene that encodes for the E3 ubiquitin ligase Parkin. Using *Caenorhabditis elegans* (*C. elegans*) as an invertebrate model that conserves the DAergic system, we previously reported significantly increased Mn accumulation in *pdr-1/parkin* mutants compared to wildtype (WT) animals. For the current study, we hypothesize that this enhanced accumulation is due to alterations in Mn transport in the *pdr-1* mutants. While no change in mRNA expression of the major Mn importer proteins (*smf-1-3*) was found in *pdr-1* mutants, significant downregulation in mRNA levels of the putative Mn exporter ferroportin (*fpn-1.1*) was observed. Using a strain overexpressing *fpn-1.1* in worms lacking *pdr-1*, we show evidence for attenuation of several endpoints of Mn-induced toxicity, including survival, metal accumulation, mitochondrial copy number and DAergic integrity, compared to *pdr-1* mutants alone. These changes suggest a novel role of *pdr-1* in modulating Mn export through altered transporter expression, and provides further support of metal dyshomeostasis as a component of Parkinsonism pathophysiology.

Introduction

Parkinson's disease (PD) is the second most common neurodegenerative disorder, with a typical age of onset around 60 years of age¹. This debilitating disease is characterized by selective dopaminergic (DAergic) cell loss in the substantia nigra pars compacta (SNpc) region of the brain. Hallmark symptoms of PD include bradykinesia, rigidity, tremors and postural instability that are often preceded by emotional instability and cognitive dysfunction. Unfortunately, PD is a progressive and irreversible condition². Current treatments do not target the molecular origins of PD, warranting further examination into the mechanisms behind its pathophysiology.

Though PD is mostly idiopathic in its etiology, mutations in several genes have been connected to the disease². For example, homozygous mutations in the *PARK2/parkin* gene are responsible for nearly 50% of an autosomal recessive, early-onset form of PD³. This gene encodes for an E3 ubiquitin ligase involved in the ubiquitin proteasome system (UPS) that targets substrates for degradation. Mutations in this gene result in impaired ligase activity and substrate binding that can lead to increased protein aggregation⁴.

^a Neuroscience Graduate Program, Vanderbilt University Medical Center, Nashville, TN, USA

^b Department of Molecular Pharmacology, Albert Einstein College of Medicine, Bronx, NY

^c Institute of Nutritional Sciences, University of Potsdam, Nuthetal, Germany

^d Department of Molecular Biology, University of Duisburg-Essen, Essen, Germany

^e Department of Neurology, Vanderbilt Kennedy Center, Center for Molecular Toxicology, Vanderbilt University Medical Center, Nashville, TN, USA

Corresponding Author:

Michael Aschner

Forchheimer 209, 1300 Morris Park Avenue, Bronx, NY

Tel: 718.430.2317, Fax: 718.430.8922

Email: Michael.Aschner@einstein.yu.edu

Parkin knockout animal models show a variety of PD-associated phenotypes, including hypokinetic deficits, DAergic cell loss and increased extracellular dopamine (DA) in the striatum^{5,6}. *Parkin* has also been more recently identified as a key regulator of mitophagy, an intracellular autophagic process designed to eliminate damaged mitochondria from the cell⁷.

Despite the known genetic associations, familial cases often present with heterogeneity in their age-of-onset and symptomatology, in addition to nearly 90% of all PD cases manifesting without genetic disturbances⁸. The idiopathic component of the disease suggests a contribution of environmental risk factors in the development of PD. One such factor is the heavy metal manganese (Mn), an essential trace element found in many food sources consumed daily by humans. Mn serves as a necessary cofactor for enzymes involved in several critical processes, including reproduction, metabolism, development, and antioxidant responses⁹. While deficiency is a rare concern, the essentiality of Mn is mirrored by its neurotoxicity upon overexposure. Mn poisoning, or manganism, typically occurs from occupational exposures in industrial settings, such as in welding, where Mn-containing fumes and/or products are abundant^{10,11}. Mn is also found as an antiknock agent methylcyclopentadienyl manganese tricarbonyl (MMT) in gasoline, but limited studies currently exist on the impact of Mn release from combustion on general human health^{12,13}. Certain pesticides also contain Mn, making surface runoff from these agricultural uses an additional source of overexposure¹. Moreover, Mn toxicity can also affect other susceptible populations, including ill neonates receiving total parenteral nutrition (TPN) that is supplemented with a trace element solution containing Mn. Intravenous TPN administration bypasses the gastrointestinal regulation of Mn absorption, resulting in 100% Mn retention⁹. Another population at risk of Mn poisoning includes patients suffering from hepatic encephalopathy and/or liver failure, as Mn is excreted from the body through the biliary system^{14,15}. On the other hand, individuals with iron (Fe) deficiency (e.g., iron deficiency anaemia), a highly prevalent nutritional condition, are at risk for increased Mn body burdens. As Mn shares similar transport mechanisms with Fe, higher Mn levels are often seen in conditions of low Fe levels¹⁶.

Tight regulation through an intricate system of transport mechanisms helps maintain proper Mn homeostasis in cells. The divalent metal transporter 1 (DMT1) represents the primary mode of divalent Mn import¹⁷. However, Mn efflux remains less understood than Mn import. We previously identified ferroportin (FPN), a well-known iron (Fe) exporter, as facilitating Mn export in cells and mice¹⁸. We have previously identified and characterized components of the Mn transport system in the *Caenorhabditis elegans* (*C. elegans*) model system. This nematode provides an attractive, alternative system that has a rapid life cycle, short lifespan, and large brood size. Additionally, the well-characterized genome allows for the utilization of various genetic mutants for studies. This nematode also conserves all necessary components of a fully functional DAergic system, allowing for the study of the effects of PD-associated genetic loss on the DAergic system. Our previous studies

have identified SMF-1, SMF-2 and SMF-3 as the *C. elegans* homologs for DMT1, with SMF3 acting as the most DMT1-like homolog in its necessity to regulate Mn uptake¹⁹. Thus far, these proteins are the only known Mn importers in the worm. Furthermore, the worm contains 3 homologs for FPN: FPN-1.1, FPN-1.2 and FPN-1.3²⁰. As of now, FPN-1.1 is the only known protein that conserves Fe efflux in *C. elegans*²¹.

The overlap in sites of damage and similar symptomatology between manganism and Parkinsonism has warranted investigations into potential gene-environment interactions. For example, *parkin* has been shown to selectively protect against Mn-induced DAergic cell death *in vitro*²², while rats exposed to Mn-containing welding fumes show increased *Parkin* protein levels²³. Our previous study using *C. elegans* found significantly enhanced Mn accumulation in *pdr-1* (*parkin* homolog) knockout worms compared to WT worms²⁴. With the aforementioned relationships between PD-associated genes and Mn toxicity, we hypothesized that this enhancement is due to an alteration in Mn homeostasis, at the level of transport, in the background of *pdr-1* loss. In the present study, while no significant change in mRNA expression of importers was seen, we found a downregulation of *fpn-1.1* mRNA. Upon overexpression of this exporter in *pdr-1* mutants, we found decreased metal levels that were associated with improved survival and DA-dependent behaviour. Together, our results provide further support for altered metal homeostasis as a component of the pathophysiology seen in Parkinsonism.

Experimental Procedures

Plasmid Constructs

Full-length wildtype (WT) *fpn-1.1* with C-terminal FLAG tag was PCR amplified using primers 5'-GGGGACAAGTTTGTACAAAAAAGCAGGCTACATGGCTTGGTTATCCGGAAAAG-3' and 5'-GGGGACCACTTTGTACAAGAAAGCTGGGTTTCACCTTGTCA TCGTCGTCCTTGTAGTCTTCAAAGTTGGCGAATCCAAC-3' from cDNA library which was converted from total RNAs isolated from N2 worms (see below). The plasmid was created with Gateway recombinational cloning (Invitrogen). The above PCR product was initially recombined with the pDONR221 vector to create the pENTRY clone. Next, the *fpn-1.1* pENTRY construct was recombined into pDEST-*sur-5* vector²⁵, under the promoter of the acetoacetyl-coenzyme A synthetase (*sur-5*) gene. This plasmid was then used to create transgenic worms.

C. elegans Strains and Strain Construction

C. elegans strains were handled and maintained at 20°C as previously described²⁶. Strains used were: N2, *wildtype* (*Caenorhabditis* Genetics Center, CGC) and VC1024, *pdr-1(gk448) III* (CGC). The MAB326 strain was created by microinjecting P_{*sur-5*}::*fpn-1.1* with pBCN27-R4R3 (P_{*rpl-28*}::PuroR, Addgene) and P_{*myo-3*}::mCherry (a gift from Dr. David Miller) into VC1024 strain. Over

three stable lines were generated and analysed. Representative lines were selectively integrated by using gamma irradiation with an energy setting of 3600 rad.

Preparation of Manganese Chloride (MnCl₂)

2 M MnCl₂ (> 99.995% purity) (Sigma-Aldrich) stock solutions were prepared in 85 mM NaCl. To prevent oxidation, fresh working solutions were prepared shortly before each experiment. The range of concentrations used in all experiments are based on Mn dose-response curves recently published by our laboratory²⁴.

Mn-Induced Treatments and Lethality Assay

2500 synchronized L1 worms per group were acutely treated with MnCl₂ (0-100 mM) in siliconized tubes for 30 minutes. Worms were then pelleted by centrifugation at 7000 rpm for 3 minutes and washed four times with 85 mM NaCl. 30-50 worms were then pre-counted and transferred to OP50-seeded NGM plates in triplicate and blinded. 48 hours post-treatment, the total number of surviving worms was scored as a percentage of the original plated worm count.

TaqMan Gene Expression Assay

Total RNA was isolated via the Trizol method. Briefly, following Mn treatment, 1 mL of Trizol (Life Technologies) was added to each tube containing 20,000 worms resuspended in 100 µl 85 mM NaCl, followed by three cycles of freezing in liquid nitrogen and thawing at 37°C. 200 µL of chloroform was then added to each tube, followed by precipitation using isopropanol and washing with 75% ethanol. Following isolation, 1 µg total RNA was used for cDNA synthesis using the High Capacity cDNA Reverse Transcription Kit (Life Technologies), per manufacturer's instructions. cDNA samples were stored at 4°C. Quantitative real-time PCR (BioRad CFX96) was conducted in duplicate wells using TaqMan Gene Expression Assay probes (Life Technologies) for each gene, using the *gpd-3* (*gapdh* homolog) housekeeping gene for normalization after determining the fold difference using the comparative 2^{-ΔΔC_T} method²⁷. The following probes were used: *smf-1* (Assay ID: Ce02496635_g1); *smf-2* (Assay ID: Ce02496634_g1); *smf-3* (Assay ID: Ce02461545_g1); *fpn-1.1* (Assay ID: Ce02414545_m1); and *gpd-3* (Assay ID: Ce02616909_gH).

Metal Quantification

Total intraworm metal content was quantified using inductively coupled plasma mass spectrometry (ICP-MS), as previously described²⁴. Briefly, 50,000 synchronized L1 worms were acutely treated with MnCl₂. Worms were then pelleted, washed five times with 85 mM NaCl and re-suspended in 1 mL 85 mM NaCl supplemented with 1% protease inhibitor. After sonication, an aliquot was taken for protein normalization using the bicinchoninic acid (BCA) assay kit (Thermo Scientific). Subsequently, the suspension was mixed again, evaporated, and incubated with the ashing mixture (65% HNO₃/30% H₂O₂ (1/1) (both Merck)) at 95 °C for at least 12 h. After dilution of the ash with bidistilled water, metal levels were determined by ICP-MS.

Relative Mitochondrial DNA Copy Number Quantification

Relative mitochondrial DNA copy number was quantified using qPCR methods as previously described²⁸, with slight modifications. Briefly, 1,000 synchronized L1 worms were treated with MnCl₂ for 30 minutes, following by several washes. Total genomic DNA was then isolated using a 1X PCR buffer containing 0.1% Proteinase K, and subjected to the following lysis protocol in a thermal cycler (BioRad T100): 65°C for 90 minutes, 95°C for 15 minutes, and then hold at 4°C. Following lysis, DNA was diluted to 3 ng/µl, and real time PCR (BioRad CFX96) using SYBR Green (BioRad) was performed in triplicate with the following primers: *nd-1* for mtDNA (forward primer sequence: 5'-AGCGTCATTTATTGGGAAGAAGAC-3'; reverse primer sequence: 5'-AAGCTTGTGCTAATCCCATAAATGT-3') and *cox-4* for nuclear DNA (forward primer sequence: 5'-GCCGACTGGAAGAACTTGTC-3'; reverse primer sequence: 5'-GCGGAGATCACC TTCCAGTA-3'). The PCR reaction consisted of: 2µL of template DNA, 1µL each of mtDNA and nucDNA primer pairs (400nM final concentration each), 12.5µL SYBR Green PCR Master Mix and 8.5µL H₂O. The following protocol was used: 50°C for 2 minutes, 95°C for 10 minutes, 40 cycles of 95°C for 15 seconds and 62°C for 60 seconds. The mitochondrial DNA content relative to nuclear DNA was calculated using the following equations: $\Delta C_T = (\text{nucDNA } C_T - \text{mtDNA } C_T)$, where relative mitochondrial DNA content = $2 \times 2^{\Delta C_T}$.

Glutathione Quantification

Total intracellular glutathione levels (reduced and oxidized GSH) have been determined using the "enzymatic recycling assay", as previously described²⁹. Briefly, whole worm extracts were prepared out of 40,000 L1 worms acutely exposed to MnCl₂. This was followed by washes with 85 mM NaCl and sonication of the pellet in 0.12 mL ice-cold extraction buffer (1% Triton X-100, 0.6% sulfosalicylic acid) and 1% protease inhibitor in KPE buffer (0.1 M potassium phosphate buffer, 5 mM EDTA). After centrifugation at 10,000 rpm for 10 minutes at 4°C, the supernatant was collected, with an aliquot reserved for protein normalization using the BCA assay. Total intracellular GSH was quantified by measuring the change in absorbance per minute at 412 nm by a microplate reader (FLUOstar Optima microplate reader, BMG Labtechnologies) after reduction of 5,5'-dithio-2-nitrobenzoic acid (DTNB, Sigma-Aldrich). Hydrogen peroxide was used as a positive control.

Basal Slowing Response Assay

This assay of dopaminergic integrity was performed as previously described³⁰, with slight modifications. Briefly, 2500 synchronized L1 worms were acutely treated in siliconized tubes with MnCl₂ for 30 minutes. Following washes with 85 mM NaCl, treated worms were transferred to seeded NGM plates. 48 hours after treatment, 60 mm NGM plates with seeded with bacteria spread in a ring (inner diameter of ~1 cm and an outer diameter of ~3.5 cm) in the center of the plate. Two seeded and two unseeded plates per group were kept at 37°C overnight, and allowed to cool to room temperature before use. Once Mn-treated animals reached the young adult stage,

1 animals were washed at least two times with S basal buffer and then
2 transferred to the central clear zone of the ring-shaped bacterial lawn
3 (5-10 worms per plate) in a drop of S basal buffer that was delicately
4 absorbed from the plate using a Kimwipe. After a five-minute
5 acclimation period, the number of body bends in a 20-second
6 interval was scored for each worm on the plate. Data are presented
7 as the change (Δ) in body bends per 20-second interval between
8 worms transferred to unseeded plates and those with bacterial rings.
9 Worms lacking *cat-2* (the homolog for tyrosine hydroxylase) were
10 used as a positive control, as these worms are impaired in bacterial
11 mechanosensation³⁰. General locomotion was assessed using the
12 number of body bends/20 seconds of the group transferred to
13 unseeded plates.
14

15 Statistics

16 Dose-response lethality curves and all histograms were generated
17 using GraphPad Prism (GraphPad Software Inc.). A sigmoidal dose-
18 response model with a top constraint at 100% was used to draw the
19 lethality curves and determine the respective LD₅₀ values, followed
20 by a one-way ANOVA with a Dunnett post-hoc test to compare all
21 strains to their respective control strains. Two-way ANOVAs were
22 performed on TaqMan gene expression, metal content, total GSH,
23 relative mtDNA copy number and basal slowing response data,
24 followed by Bonferroni's multiple comparison post-hoc tests.
25
26
27
28
29

30 Results

31 ***pdr-1* mutants show alterations in mRNA expression of Mn
32 exporter-, but not importer-related genes** - We previously
33 reported a statistically significant increase in Mn accumulation in
34 *pdr-1* mutants vs. WT worms²⁴. To test whether this enhancement
35 was due to a change in transcription of Mn importer and/or exporter
36 genes, we performed quantitative reverse transcription PCR (qRT-
37 PCR) to examine *smf-1,2,3* (Fig. 1A-1C) and *fpn-1.1* gene
38 expression (Fig. 1D), respectively, following acute Mn exposure.
39 Two-way ANOVA analysis showed no overall effect of Mn
40 treatment on transcription of any of the genes tested. However, while
41 *pdr-1* mutants showed no significant changes in *smf-1,2,3* (the
42 importers) mRNA expression (Fig. 1A-1C), a significant genotype
43 difference ($p < 0.0001$) was noted in *fpn-1.1* (the exporter) between
44 *pdr-1* mutants and WT animals. *Post-hoc* analysis revealed a
45 significant *fpn-1.1* downregulation at 0 and 2.5 mM MnCl₂ (Fig 1D).
46
47

48 **Overexpression of *fpn-1.1* in *pdr-1* mutants suppresses Mn-
49 induced lethality** - In addition to enhanced Mn accumulation, *pdr-1*
50 mutants showed a leftward shift in the Mn dose-response survival
51 curve, with WT worms exhibiting a LD₅₀ of 10.43 mM²⁴. To
52 determine whether downregulation of *fpn-1.1* may have played a
53 role in exacerbating Mn-induced lethality of *pdr-1* mutants, we
54 overexpressed *fpn-1.1* in the *pdr-1* mutant background. Upon Mn
55 exposure, *pdr-1* mutants overexpressing *fpn-1.1* (*pdr-1* KO; *fpn-1.1*
56 OVR) exhibited a rightward shift in the dose-response curve of
57 compared to *pdr-1* mutants alone (Fig. 2A). The LD₅₀ of *pdr-1* KO;
58 *fpn-1.1* OVR animals (10.84 mM) relatively normalized to
59
60

previously published WT levels, while *pdr-1* mutants alone show a
LD₅₀ of 7.416 mM (Table, 2B). Two-way ANOVA analysis showed
a significant interaction effect ($p = 0.0064$) between both genotype
and treatment ($p < 0.0001$).

**Overexpression of *fpn-1.1* in *pdr-1* mutants decreases levels of
pro-oxidant metals** - Upon noting the improved survival in *pdr-1*
KO; *fpn-1.1* OVR animals, we hypothesized that this attenuation in
Mn-induced toxicity is associated with a decrease in redox active
metal accumulation. Using inductively coupled plasma mass
spectrometry (ICP-MS), we measured intraworm concentrations of
various metals, including Mn, iron (Fe), zinc (Zn) and copper (Cu)
following acute Mn exposure. To our surprise, Mn levels remained
relatively similar between strains, though two-way ANOVA analysis
revealed a significant treatment effect ($p = 0.0165$). However,
endogenous Fe levels were significantly decreased in *pdr-1* KO; *fpn-1.1*
OVR animals compared to *pdr-1* KOs alone revealed as a
significant genotype effect by ANOVA (Fig. 3B, $p = 0.0092$). No
significant changes were seen in Zn levels (Fig. 3C). However,
similar to Fe, Cu levels were significantly decreased in *pdr-1* KO;
fpn-1.1 OVR animals compared to *pdr-1* KOs (Fig. 3D, $p = 0.0256$),
with no post-hoc level differences. In summary, Mn levels stayed
relatively the same, while Fe and Cu were both significantly
decreased in *pdr-1* KO; *fpn-1.1* OVR animals. These results indicate
that the improved survival is probably due to decreased levels of Fe
and Cu, and suggests that *fpn-1.1* may prefer Fe and Cu as substrates
over Mn.

**Overexpression of *fpn-1.1* in *pdr-1* mutants improves
mitochondrial integrity and antioxidant response** - Increased Mn
levels in *pdr-1* KOs (vs. WT animals) have been noted concurrently
with significantly increased basal levels of reactive oxygen species
(ROS) and depleted basal levels of total glutathione (GSH)²⁴,
suggesting an overall exacerbated environment of oxidative stress in
pdr-1 KO animals. Therefore, we next sought to determine whether
the significant decrease in Fe and Cu levels (Fig. 3) and
improvement in survival of *pdr-1* KO; *fpn-1.1* OVR animals (Fig. 2)
were associated with improved defence mechanisms against
oxidative stress. This was investigated using two measures: relative
mitochondrial DNA (mtDNA) copy number and total GSH levels.
Alterations in mtDNA copy number have been associated with aging
and degenerative processes³⁰. Moreover, parkin has been shown to
regulate mitochondrial turnover to maintain proper mitochondrial
integrity⁷. Using a quantitative PCR (qPCR) technique, we found
pdr-1 KO animals had a significantly elevated mtDNA copy number
relative to WT animals, whereas *pdr-1* KO; *fpn-1.1* OVR animals
exhibited levels similar to WT animals (Fig. 4A); two-way ANOVA
analysis reveals a significant genotype effect ($p = 0.0116$), though
significance was not reached at the *post-hoc* level. Moreover, we
previously published the basal depletion of total GSH in *pdr-1* KOs
compared to WT controls. Given the reversal of increased mtDNA
copy number in *pdr-1* KO; *fpn-1.1* OVR animals, we examined
whether there was a similar rescue of GSH depletion. While
statistical significance wasn't reached, there was a slight increase in
GSH levels in *pdr-1* KO; *fpn-1.1* OVR animals relative to *pdr-1* KOs
(Fig. 4C, $p = 0.09$). In both measures, Mn treatment itself did not

1 significantly affect the outcomes.

2
3 **Overexpression of *fpn-1.1* in *pdr-1* mutants improves the DA-**
4 **dependent basal slowing response** – Loss of *parkin* is connected to
5 PD-associated DAergic neurodegeneration, and we previously
6 published similar results of *pdr-1* KO's showing increased DAergic
7 neurodegeneration vs. WT worms with fluorescence microscopy²⁴.
8 Consequently, we investigated whether the visual effects of DAergic
9 neurodegeneration persisted to alter a behavioral outcome of
10 DAergic integrity. The basal slowing response is a DA-dependent
11 behavior that affects the mechanosensation needed for proper food
12 sensing in *C. elegans*, as worms slow their movement when
13 encountering a bacterial lawn. Worms lacking *cat-2*, the homolog for
14 tyrosine hydroxylase, are defective in this response from the loss of
15 dopamine synthesis and do not slow down³¹. Thus, the changes (Δ)
16 in number of body bends between plates with and without bacteria
17 reflect the integrity of DAergic neurons. Using this paradigm, *pdr-1*
18 KO animals exhibited a significantly defective basal slowing
19 response vs. WT animals ($p < 0.001$) that was analogous to that of
20 *cat-2* mutants (Fig. 5). The *pdr-1* KO;*fpn-1.1* OVR animals showed
21 a partial rescue of the response, without reaching statistical
22 significance. However, in the presence of Mn treatment, *pdr-1*
23 KO;*fpn-1.1* OVR fully restored the response to WT levels, with the
24 changes (Δ) in number of body bends being significantly higher than
25 *pdr-1* KO's alone ($p < 0.01$). To ensure that these effects were not due
26 to general locomotion differences, we compared the number of body
27 bends per group on plates without bacterial lawns; there were no
28 significant differences between all groups (data not shown).

32 Discussion

33
34 The relationship between genetic mutations and the
35 contribution of environmental risk factors in the development of PD
36 has yet to be clearly defined. In the present study, the *C. elegans*
37 model system was utilized to investigate alterations in Mn
38 homeostasis and toxicity in animals lacking *pdr-1/parkin*, a genetic
39 risk factor for PD. We previously published evidence that animals
40 lacking *pdr-1* show high sensitivity to an acute Mn exposure, with
41 decreased survival and significantly elevated Mn accumulation
42 compared to WT animals²⁴. The present study aimed to determine
43 whether the enhanced Mn concentrations were due to altered
44 expression of Mn transporters in *C. elegans* to affect Mn
45 homeostasis.

46
47 Parkin's role in regulating metal homeostasis has only
48 recently begun to be investigated. Previous *in vitro* evidence has
49 shown that parkin can modulate levels of the 1B isoform of DMT1
50 through ubiquitination³². Moreover, *Drosophila* studies show that
51 both pharmacological (BCS/BPD) or genetic (increased expression
52 of the metal responsive transcription factor 1, MTF-1) chelation of
53 redox-active metals decreases oxidative stress, improves reduced
54 lifespan and normalizes metal concentrations in *parkin* mutant
55 flies^{33, 34}. Therefore, parkin's regulation of metal homeostasis and its
56 role as an E3 ligase raise the possibility of parkin-mediated
57 regulation of Mn-responsive proteins. The *C. elegans* system

represents a ideal model to study this possibility, as PDR-1
conserves its ligase activity³⁵, and their genome contains less E3
ligases³⁶ to minimize the possible compensatory mechanisms seen in
vertebrate knockout models.

The enhanced Mn accumulation in *pdr-1* mutant animals
may be a selective phenotype of this particular genetic background.
Notably, our previous studies using methylmercury (MeHg)
exposure do not show the same accumulation phenotypes in *pdr-1*
KO's³⁷. Moreover, Aboud *et al.* showed increased oxidative stress
in response to Mn exposure in neuroprogenitor cells from patients
possessing *parkin* mutations, despite exhibiting reduced Mn
accumulation³⁸, which is opposite to our ICP-MS findings. This
discrepancy may be due to their human data arising from isolated
neuroprogenitors, whereas the current study assesses whole-worm
Mn levels. Nonetheless, such studies provide further support of
alterations in neuronal Mn biology in the presence of *parkin*
mutations. This may be true for other PD genetic risk factors as well,
as recent studies have highlighted the role of another PD-linked gene
known as *PARK9*, which encodes for the P-type ATPase ion pump
ATP13A2. Evidence shows that this protein modulates Zn
homeostasis³⁹, with previous evidence indicating that this protein
can also transport Mn⁴⁰. However, our findings with the *pdr-1*
mutant background show no differences in Zn accumulation,
providing further support for a selective relationship between Parkin
and Mn homeostasis.

Contrary to *in vitro* evidence of parkin-mediated control of
a DMT isoform, we observed no significant changes in expression of
the *smf* genes, especially with *smf-3* being the most DMT1-like
homolog¹⁹. Instead, significant downregulation of *fpn-1.1* was
observed in *pdr-1* KO's compared to WT animals. These findings
suggest that the loss of *pdr-1* in *C. elegans* results in increased Mn
accumulation from defective export, rather than from impaired
uptake. Notably, we recently identified a novel role for SLC30A10
in Mn export that is associated with heightened risk for PD.
However, no homologs for this protein are expressed in *C. elegans*⁴¹.
Thus, for the present study, given the downregulation of *fpn-1.1*
mRNA in *pdr-1* mutants, we investigated whether overexpression of
the only known Mn exporter in *C. elegans* would result in a rescue
of *pdr-1* mutant phenotypes.

Mn uptake is modulated by a variety of proteins,
including: DMT1, the transferrin receptor (TfR), the choline
transporter, the citrate transporter, the magnesium transporter HIP14,
ATP13A2, the solute carrier 39 family of zinc transporters, and
calcium channels¹⁰. Among these, DMT1 has been given the most
attention, as it is not only the primary mode of uptake, but is also
associated with parkinsonism. Increased DMT1 expression has been
found in the SNpc of PD patients, as well as in SNpc of MPTP
mouse models⁴². Elevated DMT1 mRNA expression and DAergic
neurotoxicity was also seen in rats exposed to Mn-containing
welding fumes⁴³. Moreover, specific polymorphisms in DMT1 have
been found in a Chinese population suffering from PD⁴⁴. These
studies highlight altered metal homeostasis in the etiology of
Parkinsonism. Interestingly, the overexpression of FPN in our *pdr-1*
mutants altered not only Mn, but Fe and Cu levels to a greater

1 extent. We were not surprised to observe a treatment effect for Mn,
2 as this was the only exogenous treatment administered to the
3 nematodes. However, we did expect to see a greater decrease in Mn
4 concentrations. It is possible that FPN's affinity for Fe is greater
5 than that of Mn, as the differential binding affinities have yet to be
6 determined. Moreover, as FPN has not been shown to export Cu, the
7 decrease in Cu levels may be a secondary effect of lowered
8 intracellular Fe due to increased Fe efflux. Fe-deficiency anaemia
9 has been associated with copper deficiencies, though the mechanism
10 remains unknown^{45, 46}. Though future studies are needed to further
11 elucidate FPN's transport profile in *C. elegans*, the rescue of the *pdr-1*
12 mutant phenotype through FPN overexpression supports our
13 hypothesis that metal dyshomeostasis in the background of *pdr-1*
14 loss may be due to alterations in transporter expression.

15
16 In addition to the well-characterized toxicity of Mn
17 resulting in Parkinsonian symptoms, enhanced iron accumulation in
18 the SN is often seen in PD brains^{42, 47}, with pharmacological Fe
19 chelation showing potential therapeutic value^{48, 49}. Moreover, Mn
20 treatment has been recently shown to disrupt general metal
21 homeostasis in WT *C. elegans*, with excess Mn resulting in altered
22 Fe and Cu levels⁵⁰. Though the authors of this study used slightly
23 higher Mn concentrations (10-30 mM) than the present study, this
24 was most likely due to the use of older worms treated for 24 hours,
25 rather than larval stage worms acutely treated for 30 minutes.
26 However, as their lowest dose (10 mM) is within the range of the
27 doses used in the present study, similar findings were seen with
28 higher Mn concentrations (30 mM) corresponding with
29 comparatively lower Fe and Cu levels overall⁵⁰. The results in the
30 present study provide further support of the interplay between
31 metals, as exogenous Mn treatment results in the alteration of
32 endogenous metal concentrations that may alter vital downstream
33 processes. It is possible that the combined effects of decreased Fe
34 and Cu levels, rather than the moderate to slight decrease in Mn
35 levels, results in the amelioration of the *pdr-1* KO phenotypes.
36 Moreover, the connection between Cu and a mutant *parkin*
37 background is further supported by recent human data showing
38 increased Cu sensitivity in neuroprogenitors from patients carrying
39 *PARK2* mutations⁵¹.

40
41 The recently discovered role of parkin as a mediator of
42 mitophagy has introduced the potential significance of mitochondrial
43 integrity in Parkinsonism⁵²; loss of *parkin* could result in the
44 accumulation of defective mitochondria to increase cellular
45 oxidative stress. This could explain the significant increase in
46 relative mtDNA copy number in *pdr-1* KO animals as a measure that
47 could equate with increased mitochondrial mass in *pdr-1* KOs. This
48 data corresponds with our previously published findings that *pdr-1*
49 KOs exhibit significantly increased ROS levels²⁴. Notably, it seems
50 controversial in the literature whether increased mtDNA copy
51 number is protective or damaging in degenerative processes^{53, 54}.
52 However, increased mtDNA copy number has been associated with
53 aging, as well as a response to increased oxidative stress³⁰.
54 Therefore, the increased copy number may also be in response to
55 increased oxidative stress from enhanced Mn accumulation to
56 compensate for damaged mitochondria. This may be especially true

57 due to the preferential accumulation of Mn in mitochondria⁵⁵.
58 Consequently, the beneficial alterations in Mn, Fe and Cu in *pdr-1*
59 KO;*fpn-1.1* OVR animals would then help to reverse this effect by
60 decreasing metal-induced oxidative stress. Additionally, the increase
in the antioxidant GSH in *pdr-1* KO;*fpn-1.1* OVR animals vs. *pdr-1*
KO animals is modest, though it does not reach statistical
significance. This may represent a slight improvement in the overall
handling of oxidative stress. It has been previously shown that
neurons treated with increasing Fe concentrations show depletion in
GSH content⁵⁶. This is similar to the elevation in GSH content of
pdr-1 KO;*fpn-1.1* OVR animals that also exhibit decreased Fe
accumulation. However, we are limited in the present study, as we
have been unsuccessful in using the microplate assay format to
measure both GSSG and GSH. While *pdr-1* KO;*fpn-1.1* OVR and
pdr-1 KO animals show no difference in *gcs-1* (homolog for the
glutamate-cysteine ligase responsible for catalysing GSH synthesis)
mRNA expression (data not shown), future studies should be done to
determine whether this change in GSH is due to more reduced vs.
oxidized forms of GSH.

Finally, we previously reported that *pdr-1* KO animals
show an exacerbation of DAergic neurodegeneration compared to
WT animals²⁴. Currently, conflicting findings exist on the effects of
Mn on DAergic neurodegeneration in *C. elegans*^{50, 57}. However, this
may be due to differences in treatment paradigms and doses.
Additionally, fluorescence microscopy is a common technique to
assess degeneration; however, microscopy for GFP visualization
remains a mostly qualitative readout of cell death. Accordingly, we
focused on an output parameter of an intact DAergic system by
assaying a DA-dependent behavioural measure. The basal slowing
response (BSR) is a well-known feeding response that requires DA
and affects mechanosensation to properly recognize food sources
(bacteria) in *C. elegans*³¹. Similar to our previous results²⁴, Mn
treatment itself in WT animals did not result in a statistically
significant decrease in BSR, though a slight decline was apparent.
However, while *pdr-1* KOs show impairment in this response, the
rescue of BSR deficits by *pdr-1* KO;*fpn-1.1* OVR animals
normalizes to the WT response. These data suggest that the
overexpression of FPN normalizes DAergic integrity in the
background of *pdr-1* loss. The effect of Mn on BSR in *pdr-1* KO
and *pdr-1* KO;*fpn-1.1* OVR animals is negligible. This may be due to
the complete loss of *pdr-1* resulting in a "ceiling effect," such that
the addition of Mn exposure does not further exacerbate the basal
differences. However, the BSR in *pdr-1* KO;*fpn-1.1* OVR animals
fully normalizes to WT levels upon treatment.

Notably, we cannot relate the improvement in BSR to the
improved survival of *pdr-1* KO;*fpn-1.1* OVR animals, as it has been
previously reported that ablation of DAergic neurons in nematodes
does not affect overall survival⁵⁸. However, the relationship between
metals and dopamine toxicity is well known. Dopamine itself is a
strong oxidant that can undergo an auto-oxidation process to produce
highly damaging intermediates, which makes a strong argument for
the vulnerability of DA-specific brain areas to toxins and other
oxidants⁵⁹. Mn has been shown to catalyse dopamine oxidation⁶⁰,
while Fe has been shown to specifically bind neuromelanin found in

1 DAergic neurons⁶¹. Thus, the *pdr-1* KO; *fpn-1.1* OVR animals may
 2 show improvement in the DA-dependent BSR due to the lower
 3 bioavailability of Mn, Fe and Cu that would otherwise participate in
 4 directly enhancing DA oxidation and/or indirectly producing
 5 damaging free radicals in an already susceptible cell type.
 6

7 Conclusion

8 In conclusion, the present study provides further support
 9 for altered metal homeostasis as a critical component of PD
 10 pathophysiology. Using the genetically tractable *C. elegans* system,
 11 we show a novel role of *pdr-1/parkin* in modulating metal
 12 homeostasis following an acute Mn exposure, affecting metal efflux.
 13 Though human mutations in FPN have not yet been associated with
 14 PD, our findings demonstrate the importance and specificity of PD
 15 genetics (e.g. loss of *pdr-1/parkin*) in interacting with environmental
 16 factors to exacerbate physiological processes that may lead to cell
 17 death. Future studies should focus on potential therapeutic routes
 18 that help understand the interplay between *pdr-1/parkin*-mediated
 19 mitochondrial dynamics and enhanced efflux of redox-active metals
 20 like Mn, Fe and Cu as a strategy against Mn-induced Parkinsonism.
 21

22 Acknowledgements

23 This work was funded by the NIH grant R01 ES10563, the Josef
 24 Schormüller Award and the DFG (BO 4103/1-1). We would also
 25 like to thank the Miller laboratory (Vanderbilt University Medical
 26 Center) for sharing resources. Lastly, we would like to thank the
 27 laboratories of Drs. Bill Valentine, Keith Erikson and Joel Meyer for
 28 scientific communications.
 29

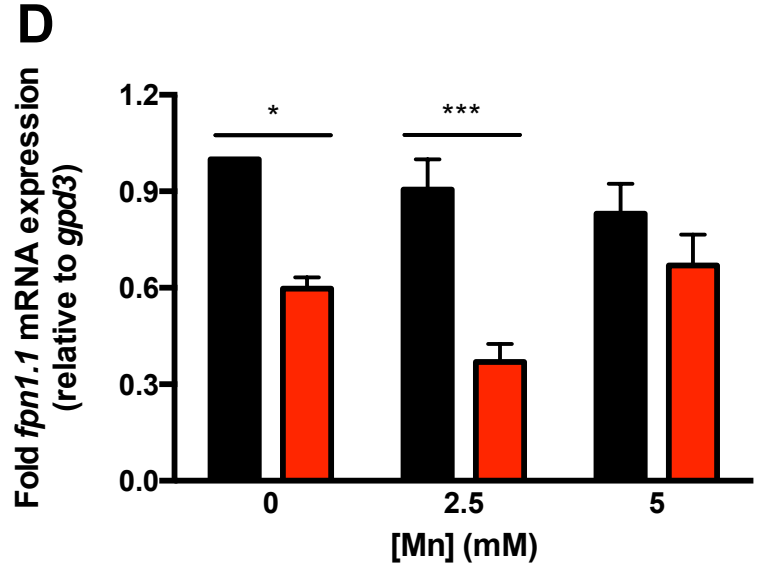
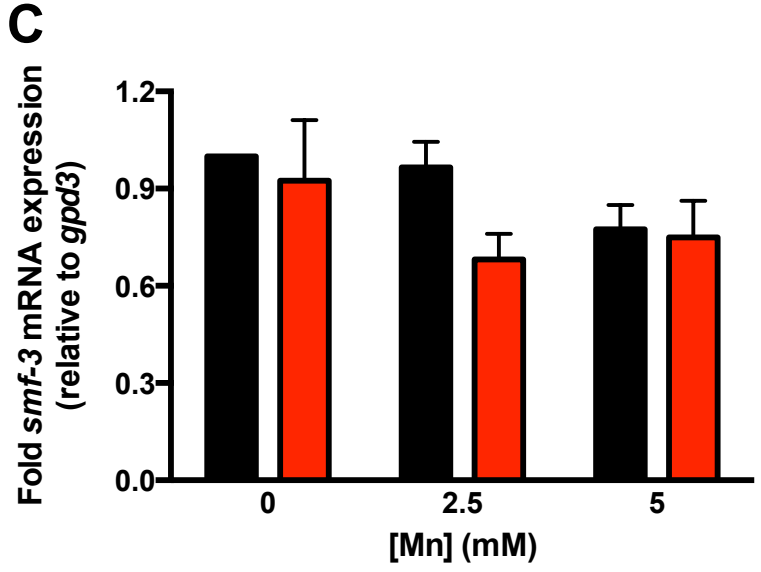
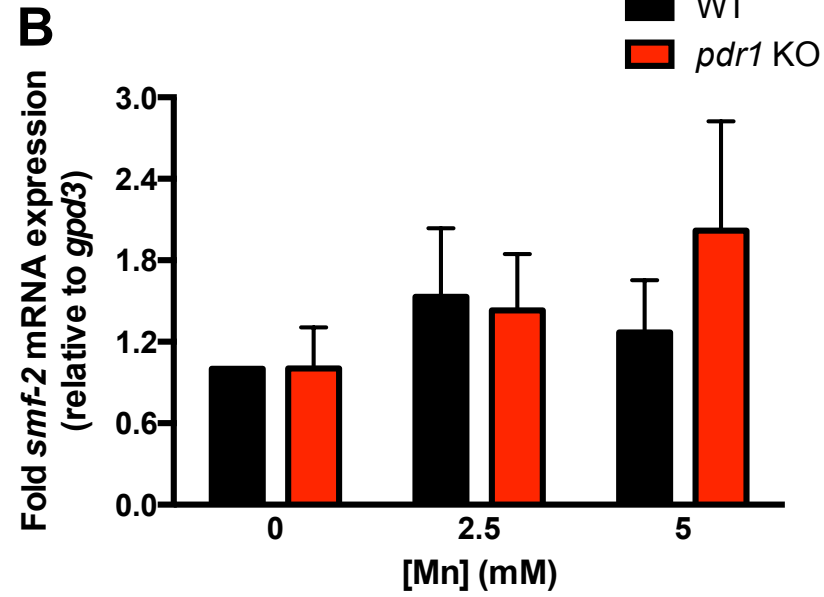
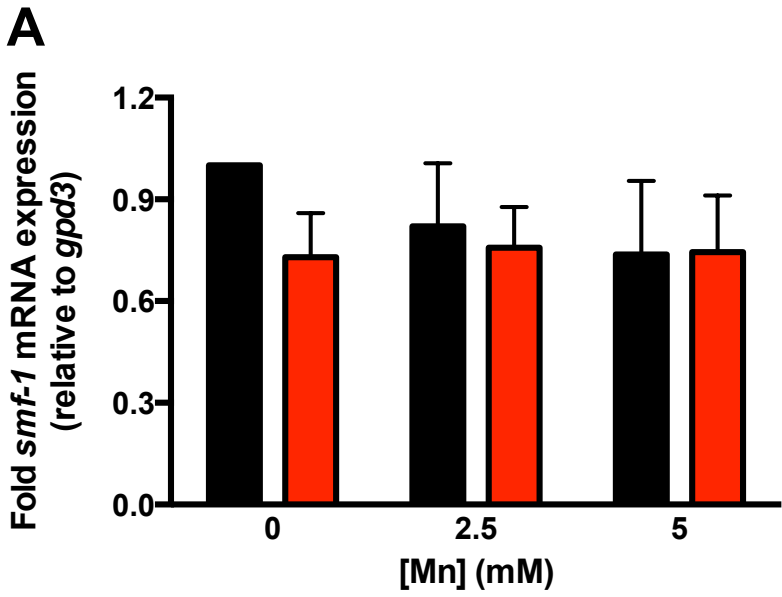
30 References

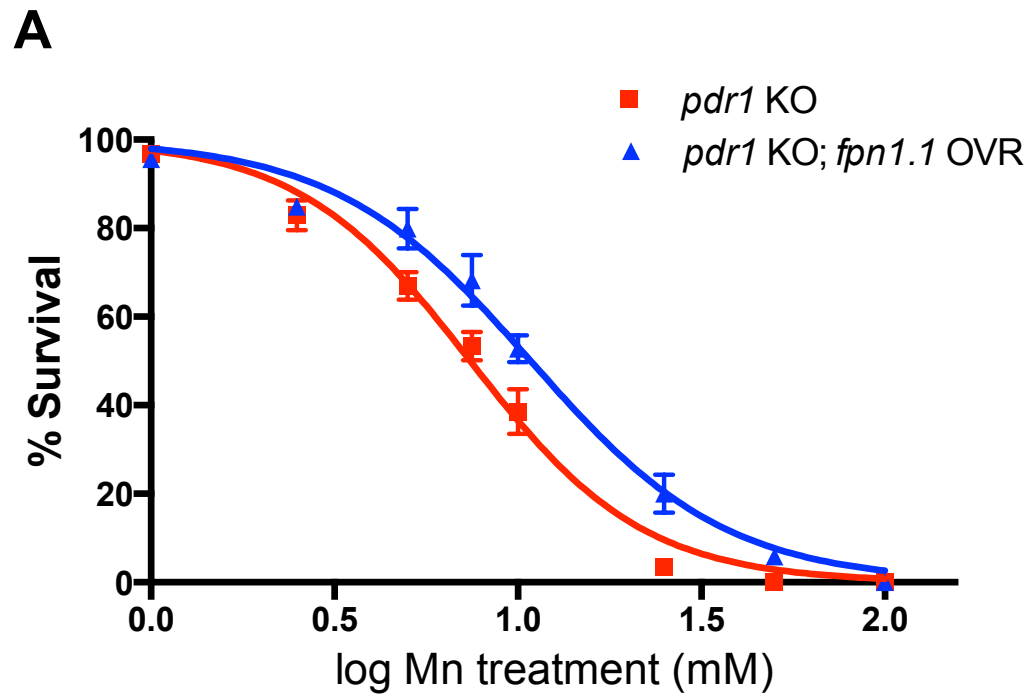
- 31 1. ATSDR, *U.S. Department of Health and Human Services, Public*
 32 *Service*, 2008.
- 33 2. A. J. Lees, J. Hardy and T. Revesz, *Lancet*, 2009, 373, 2055-2066.
- 34 3. T. Kitada, S. Asakawa, N. Hattori, H. Matsumine, Y. Yamamura, S.
 35 Minoshima, M. Yokochi, Y. Mizuno and N. Shimizu, *Nature*,
 36 1998, 392, 605-608.
- 37 4. S. R. Sriram, X. Li, H. S. Ko, K. K. Chung, E. Wong, K. L. Lim, V.
 38 L. Dawson and T. M. Dawson, *Human molecular genetics*,
 39 2005, 14, 2571-2586.
- 40 5. T. K. Sang, H. Y. Chang, G. M. Lawless, A. Ratnaparkhi, L. Mee, L.
 41 C. Ackerson, N. T. Maidment, D. E. Krantz and G. R. Jackson,
 42 *The Journal of neuroscience : the official journal of the Society*
 43 *for Neuroscience*, 2007, 27, 981-992.
- 44 6. M. S. Goldberg, S. M. Fleming, J. J. Palacino, C. Cepeda, H. A. Lam,
 45 A. Bhatnagar, E. G. Meloni, N. Wu, L. C. Ackerson, G. J.
 46 Klapstein, M. Gajendiran, B. L. Roth, M. F. Chesselet, N. T.
 47 Maidment, M. S. Levine and J. Shen, *The Journal of biological*
 48 *chemistry*, 2003, 278, 43628-43635.

- 49 7. C. Vives-Bauza, C. Zhou, Y. Huang, M. Cui, R. L. de Vries, J. Kim,
 50 J. May, M. A. Tocilescu, W. Liu, H. S. Ko, J. Magrane, D. J.
 51 Moore, V. L. Dawson, R. Grailhe, T. M. Dawson, C. Li, K.
 52 Tieu and S. Przedborski, *Proceedings of the National Academy*
 53 *of Sciences of the United States of America*, 2010, 107, 378-
 54 383.
- 55 8. J. Blesa, S. Phani, V. Jackson-Lewis and S. Przedborski, *Journal of*
 56 *biomedicine & biotechnology*, 2012, 2012, 845618.
- 57 9. J. L. Aschner and M. Aschner, *Molecular aspects of medicine*, 2005,
 58 26, 353-362.
- 59 10. M. Aschner, K. M. Erikson, E. Herrero Hernandez and R. Tjalkens,
 60 *Neuromolecular medicine*, 2009, 11, 252-266.
11. K. Tuschl, P. B. Mills and P. T. Clayton, *International review of*
neurobiology, 2013, 110, 277-312.
12. A. K. Bhuie, O. A. Ogunseitan, R. R. White, M. Sain and D. N. Roy,
The Science of the total environment, 2005, 339, 167-178.
13. M. M. Finkelstein and M. Jerrett, *Environmental research*, 2007, 104,
 420-432.
14. H. M. Zeron, M. R. Rodriguez, S. Montes and C. R. Castaneda,
Journal of trace elements in medicine and biology : organ of
the Society for Minerals and Trace Elements, 2011, 25, 225-
 229.
15. K. J. Klos, J. E. Ahlskog, K. A. Josephs, R. D. Fealey, C. T. Cowl
 and N. Kumar, *Archives of neurology*, 2005, 62, 1385-1390.
16. E. A. Smith, P. Newland, K. G. Bestwick and N. Ahmed, *Journal of*
trace elements in medicine and biology : organ of the Society
for Minerals and Trace Elements, 2013, 27, 65-69.
17. M. D. Garrick, K. G. Dolan, C. Horbinski, A. J. Ghio, D. Higgins, M.
 Porubcin, E. G. Moore, L. N. Hainsworth, J. N. Umbreit, M. E.
 Conrad, L. Feng, A. Lis, J. A. Roth, S. Singleton and L. M.
 Garrick, *Biomaterials : an international journal on the role of*
metal ions in biology, biochemistry, and medicine, 2003, 16,
 41-54.
18. Z. Yin, H. Jiang, E. S. Lee, M. Ni, K. M. Erikson, D. Milatovic, A. B.
 Bowman and M. Aschner, *Journal of neurochemistry*, 2010,
 112, 1190-1198.
19. C. Au, A. Benedetto, J. Anderson, A. Labrousse, K. Erikson, J. J.
 Ewbank and M. Aschner, *PLoS one*, 2009, 4, e7792.
20. C. P. Anderson and E. A. Leibold, *Frontiers in pharmacology*, 2014,
 5, 113.
21. I. De Domenico, E. Lo, B. Yang, T. Korolnek, I. Hamza, D. M. Ward
 and J. Kaplan, *Cell metabolism*, 2011, 14, 635-646.
22. Y. Higashi, M. Asanuma, I. Miyazaki, N. Hattori, Y. Mizuno and N.
 Ogawa, *Journal of neurochemistry*, 2004, 89, 1490-1497.
23. K. Sriram, G. X. Lin, A. M. Jefferson, J. R. Roberts, O. Wirth, Y.
 Hayashi, K. M. Krajnak, J. M. Soukup, A. J. Ghio, S. H.
 Reynolds, V. Castranova, A. E. Munson and J. M. Antonini,
FASEB journal : official publication of the Federation of
American Societies for Experimental Biology, 2010, 24, 4989-
 5002.
24. J. Bornhorst, S. Chakraborty, S. Meyer, H. Lohren, S. G. Brinkhaus,
 A. L. Knight, K. A. Caldwell, G. A. Caldwell, U. Karst, T.
 Schwerdtle, A. Bowman and M. Aschner, *Metallomics :*
integrated biometal science, 2014, 6, 476-490.
25. D. Leyva-Illades, P. Chen, C. E. Zogzas, S. Hutchens, J. M. Mercado,
 C. D. Swaim, R. A. Morrisett, A. B. Bowman, M. Aschner and

- 1 S. Mukhopadhyay, *The Journal of Neuroscience*, 2014, 34,
2 14079-14095.
- 3 26. S. Brenner, *Genetics*, 1974, 77, 71-94.
- 4 27. K. J. Livak and T. D. Schmittgen, *Methods*, 2001, 25, 402-408.
- 5 28. S. E. Hunter, D. Jung, R. T. Di Giulio and J. N. Meyer, *Methods*,
6 2010, 51, 444-451.
- 7 29. I. Rahman, A. Kode and S. K. Biswas, *Nature protocols*, 2006, 1,
8 3159-3165.
- 9 30. H. C. Lee, P. H. Yin, C. Y. Lu, C. W. Chi and Y. H. Wei, *The*
10 *Biochemical journal*, 2000, 348 Pt 2, 425-432.
- 11 31. E. R. Sawin, R. Ranganathan and H. R. Horvitz, *Neuron*, 2000, 26,
12 619-631.
- 13 32. J. A. Roth, S. Singleton, J. Feng, M. Garrick and P. N. Paradkar,
14 *Journal of neurochemistry*, 2010, 113, 454-464.
- 15 33. N. Saini, O. Georgiev and W. Schaffner, *Molecular and cellular*
16 *biology*, 2011, 31, 2151-2161.
- 17 34. N. Saini, S. Oelhafen, H. Hua, O. Georgiev, W. Schaffner and H.
18 Bueler, *Neurobiology of disease*, 2010, 40, 82-92.
- 19 35. W. Springer, T. Hoppe, E. Schmidt and R. Baumeister, *Human*
20 *molecular genetics*, 2005, 14, 3407-3423.
- 21 36. N. Papaevgeniou and N. Chondrogianni, *Redox biology*, 2014, 2,
22 333-347.
- 23 37. E. J. Martinez-Finley, S. Chakraborty, J. C. Slaughter and M.
24 Aschner, *Neurochemical research*, 2013, 38, 1543-1552.
- 25 38. A. A. Aboud, A. M. Tidball, K. K. Kumar, M. D. Neely, K. C. Ess,
26 K. M. Erikson and A. B. Bowman, *Neurotoxicology*, 2012, 33,
27 1443-1449.
- 28 39. S. M. Kong, B. K. Chan, J. S. Park, K. J. Hill, J. B. Aitken, L. Cottle,
29 H. Farghaian, A. R. Cole, P. A. Lay, C. M. Sue and A. A.
30 Cooper, *Human molecular genetics*, 2014, 23, 2816-2833.
- 31 40. A. Chesi, A. Kilaru, X. Fang, A. A. Cooper and A. D. Gitler, *PloS*
32 *one*, 2012, 7, e34178.
- 33 41. D. Leyva-Illades, P. Chen, C. E. Zogzas, S. Hutchens, J. M. Mercado,
34 C. D. Swaim, R. A. Morrisett, A. B. Bowman, M. Aschner and
35 S. Mukhopadhyay, *The Journal of neuroscience : the official*
36 *journal of the Society for Neuroscience*, 2014, 34, 14079-
37 14095.
- 38 42. J. Salazar, N. Mena, S. Hunot, A. Prigent, D. Alvarez-Fischer, M.
39 Arredondo, C. Duyckaerts, V. Sazdovitch, L. Zhao, L. M.
40 Garrick, M. T. Nunez, M. D. Garrick, R. Raisman-Vozari and
41 E. C. Hirsch, *Proceedings of the National Academy of Sciences*
42 *of the United States of America*, 2008, 105, 18578-18583.
- 43 43. K. Sriram, G. X. Lin, A. M. Jefferson, J. R. Roberts, R. S. Chapman,
44 B. T. Chen, J. M. Soukup, A. J. Ghio and J. M. Antonini,
45 *Archives of toxicology*, 2010, 84, 521-540.
- 46 44. Q. He, T. Du, X. Yu, A. Xie, N. Song, Q. Kang, J. Yu, L. Tan, J. Xie
47 and H. Jiang, *Neuroscience letters*, 2011, 501, 128-131.
- 48 45. J. R. Prohaska and M. Broderius, *Biomaterials : an international journal*
49 *on the role of metal ions in biology, biochemistry, and*
50 *medicine*, 2012, 25, 633-642.
- 51 46. J. R. Prohaska, *Annals of the New York Academy of Sciences*, 2014,
52 1314, 1-5.
- 53 47. S. Ayton, P. Lei, P. A. Adlard, I. Volitakis, R. A. Cherny, A. I. Bush
54 and D. I. Finkelstein, *Molecular neurodegeneration*, 2014, 9,
55 27.
- 56 48. R. B. Mounsey and P. Teismann, *International journal of cell*
57 *biology*, 2012, 2012, 983245.
- 58 49. D. Ben-Shachar, G. Eshel, P. Riederer and M. B. Youdim, *Annals of*
59 *neurology*, 1992, 32 Suppl, S105-110.
- 60 50. S. Angeli, T. Barhydt, R. Jacobs, D. W. Killilea, G. J. Lithgow and J.
K. Andersen, *Metallomics : integrated biometal science*, 2014,
6, 1816-1823.
51. A. A. Aboud, A. M. Tidball, K. K. Kumar, M. D. Neely, B. Han, K.
C. Ess, C. C. Hong, K. M. Erikson, P. Hedera and A. B.
Bowman, *Neurobiology of disease*, 2014, 73C, 204-212.
52. R. L. de Vries and S. Przedborski, *Molecular and cellular*
neurosciences, 2013, 55, 37-43.
53. P. Podlesniy, J. Figueiro-Silva, A. Llado, A. Antonell, R. Sanchez-
Valle, D. Alcolea, A. Lleo, J. L. Molinuevo, N. Serra and R.
Trullas, *Annals of neurology*, 2013, 74, 655-668.
54. F. Gu, V. Chauhan, K. Kaur, W. T. Brown, G. LaFauci, J. Wegiel
and A. Chauhan, *Translational psychiatry*, 2013, 3, e299.
55. C. E. Gavin, K. K. Gunter and T. E. Gunter, *Neurotoxicology*, 1999,
20, 445-453.
56. P. Aracena, P. Aguirre, P. Munoz and M. T. Nunez, *Biological*
research, 2006, 39, 157-165.
57. A. Benedetto, C. Au, D. S. Avila, D. Milatovic and M. Aschner,
PLoS genetics, 2010, 6.
58. R. Nass, D. H. Hall, D. M. Miller, 3rd and R. D. Blakely,
Proceedings of the National Academy of Sciences of the United
States of America, 2002, 99, 3264-3269.
59. R. Graumann, I. Paris, P. Martinez-Alvarado, P. Rumanque, C.
Perez-Pastene, S. P. Cardenas, P. Marin, F. Diaz-Grez, R.
Caviedes, P. Caviedes and J. Segura-Aguilar, *Polish journal of*
pharmacology, 2002, 54, 573-579.
60. C. D. Garner and J. P. Nachtman, *Chemico-biological interactions*,
1989, 69, 345-351.
61. M. G. Bridelli, D. Tampellini and L. Zecca, *FEBS letters*, 1999, 457,
18-22.

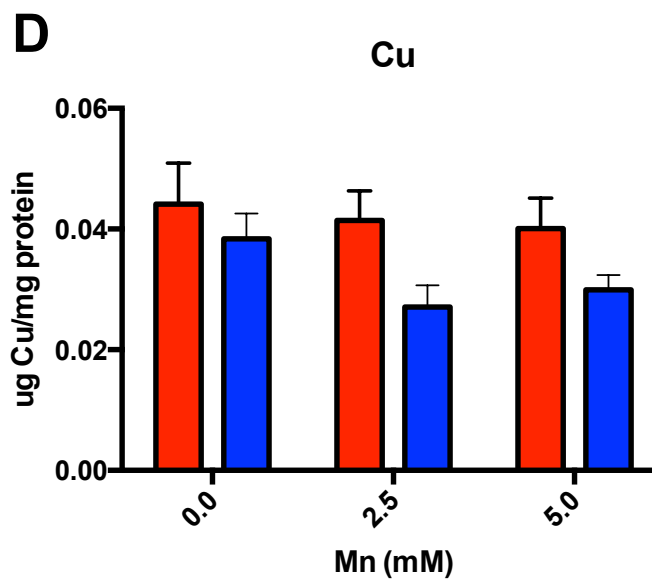
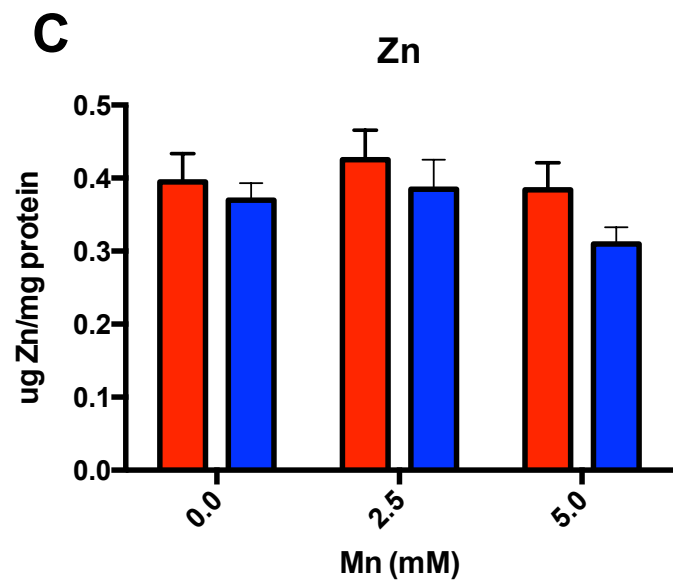
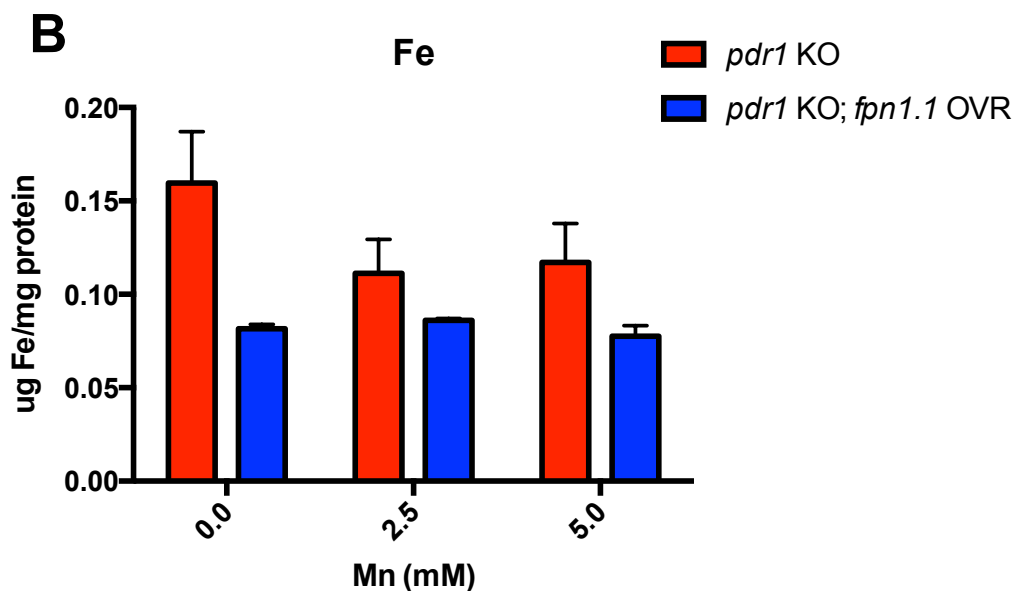
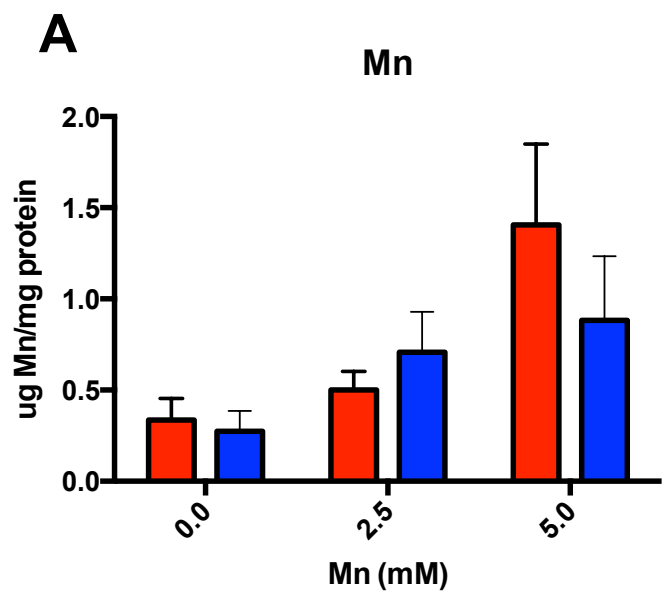
1
2
3
4
5
6
7
8
9
10
11
12
13
14
15
16
17
18
19
20
21
22
23
24
25
26
27
28
29
30
31
32
33
34
35
36
37
38
39
40
41
42
43
44
45
46
47
48
49

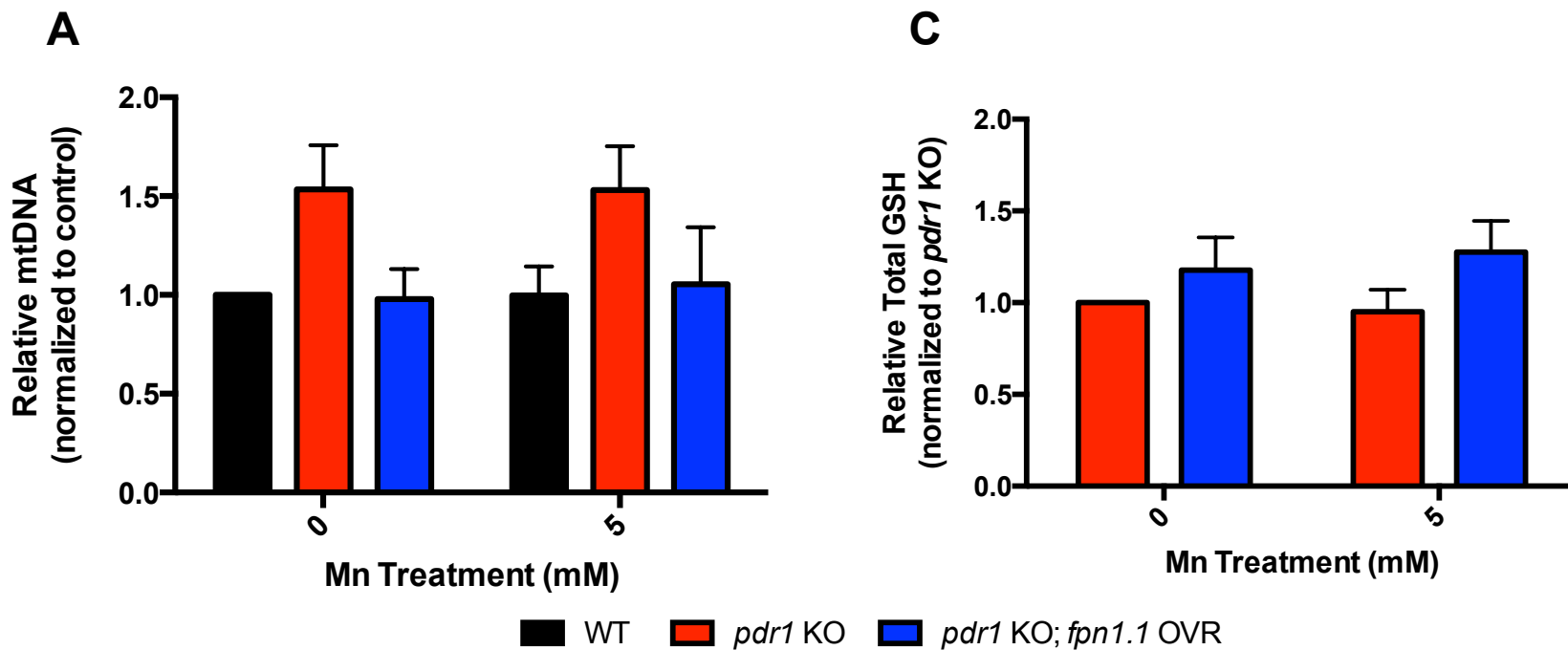




B

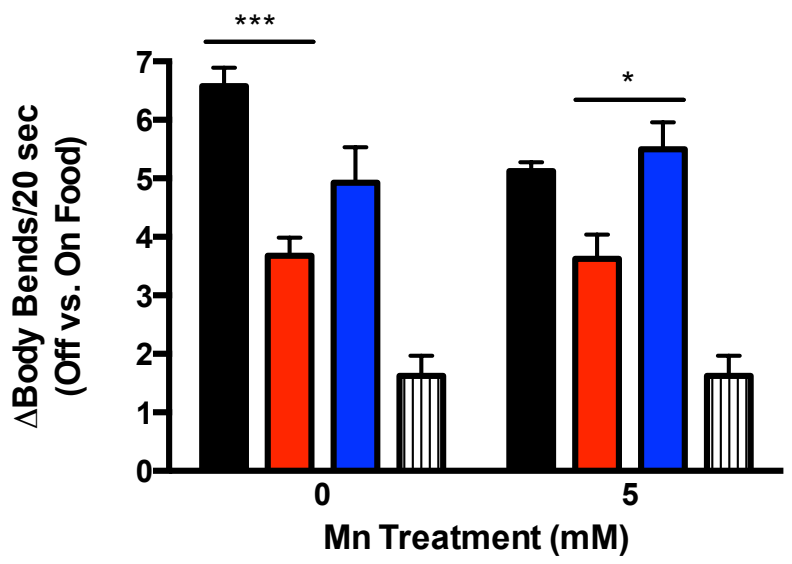
Strain	Genotype	LD ₅₀ (mM MnCl ₂)
VC1024	<i>pdr1(gk448) III</i> (KO)	7.416
MAB326	<i>pdr1(gk448) III</i> (KO); <i>fpn1.1</i> OVR	10.84



**B**

Source of Variation	p-value
Interaction	<i>0.9747</i>
Treatment	<i>0.8816</i>
Genotype	<i>0.0116</i>

1
2
3
4
5
6
7
8
9
10
11
12
13
14
15
16
17
18
19
20
21
22
23
24
25
26
27
28
29
30
31
32
33
34
35
36
37
38
39
40
41
42
43
44
45
46
47
48
49



■ WT ■ pdr1 KO ■ pdr1 KO; fpn1.1 OVR ■ cat-2 KO



FIGURE LEGENDS

FIGURE 1. *pdr-1* mutants show alterations in mRNA expression of Mn exporter, but not importer, genes. (A-D) *smf-1,2,3* and *fpn-1.1* mRNA expression after an acute, 30 min treatment of L1 worms with 0, 2.5 and 5 mM MnCl₂. Relative gene expression was determined by qRT-PCR. (A) *smf-1* mRNA expression in N2 (WT) and *pdr-1* KO animals. (B) *smf-2* mRNA expression in N2 (WT) and *pdr-1* KO animals. (C) *smf-3* mRNA expression in N2 (WT) and *pdr-1* KO animals. (D) *fpn-1.1* mRNA expression in N2 (WT) and *pdr-1* KO animals. (A-D) Data are expressed as mean values + SEM of at least five independent experiments in duplicates normalized to the untreated wildtype and relative to *gpd3* mRNA. Statistical analysis by two-way ANOVA: (A) interaction, ns; genotype, ns; concentration, ns; (B) interaction, ns; genotype, ns; concentration, ns; (C) interaction, ns; genotype, ns; concentration, ns; (D) interaction, ns (trend level, p=0.0639); genotype, p<0.0001; concentration, ns. *p < 0.05, ***p < 0.001 vs. respective wildtype worms.

FIGURE 2. Overexpression of *fpn-1.1* in *pdr-1* mutants rescues Mn-induced lethality. (A,B) Dose-response survival curves following acute Mn exposure. All values were compared to untreated worms set to 100% survival and plotted against the logarithmic scale of the used Mn concentrations. (A) *pdr-1* KO animals and *pdr-1* mutants overexpressing *fpn-1.1* (*pdr-1* KO; *fpn-1.1* OVR) were treated at the L1 stage for 30 min with increasing MnCl₂ concentrations. (B) The respective LD₅₀ concentrations (mM MnCl₂) for both genotypes. Data are expressed as mean values + SEM from at least five independent experiments. Statistical analysis by two-way ANOVA: interaction, p=0.0064; genotype, p<0.0001; concentration, p<0.0001.

FIGURE 3. Overexpression of *fpn-1.1* in *pdr-1* mutants decreases levels of highly pro-oxidant metals. (A-D) Intraworm metal concentrations following acute, 30 min MnCl₂ treatment (0, 2.5 and 5 mM) at the L1 stage, as quantified by ICP-MS/MS. (A) Mn content (µg Mn/mg protein) in *pdr-1* KO and *pdr-1* KO; *fpn-1.1* OVR animals. (B) Iron (Fe) content (µg Fe/mg protein) in *pdr-1* KO and *pdr-1* KO; *fpn-1.1* OVR animals. (C) Zinc (Zn) content (µg Zn/mg protein) in *pdr-1* KO and *pdr-1* KO; *fpn-1.1* OVR animals. (D) Copper (Cu) content (µg Cu/mg protein) in *pdr-1* KO and *pdr-1* KO; *fpn-1.1* OVR animals. (A-D) Data are expressed as mean values + SEM from at least six independent experiments and normalized to total protein content. Statistical analysis by two-way ANOVA: (A) interaction, ns; genotype, ns; concentration, p=0.0165; (B) interaction, ns; genotype, p=0.0092; concentration, ns; (C) interaction, ns; genotype, ns; concentration, ns; (D) interaction, ns; genotype, p=0.0256; concentration, ns.

FIGURE 4. Overexpression of *fpn-1.1* in *pdr-1* mutants improves mitochondrial integrity and antioxidant response. (A) Relative mitochondrial DNA (mtDNA) copy number in *pdr-1* KO and *pdr-1* KO; *fpn-1.1* OVR animals following an acute, 30 min treatment with 0 and 5 mM MnCl₂. Relative gene expression was determined by qPCR. (B) Two-way ANOVA analysis of data in 4A showing genotype significance in mtDNA copy number. (C) Total glutathione (GSH) levels of *pdr-1* KO and *pdr-1* KO; *fpn-1.1* OVR animals following an acute, 30 min treatment with 0 and 5 mM MnCl₂. (A) Relative mtDNA copy

1
2
3 number is expressed as a ratio of *nd-1* (mtDNA marker) to *cox-4* (nuclear DNA marker). Data are
4 expressed as mean values + SEM of at least five independent experiments in duplicates normalized to the
5 untreated N2 wildtype values. (C) Data are expressed as mean values + SEM of at least five independent
6 experiments in duplicates, normalized to total protein content and relative to untreated *pdr-1* KO values.
7 Statistical analysis by two-way ANOVA: (A) interaction, ns; genotype, $p=0.0116$; concentration, ns; (B)
8 interaction, ns; genotype, ns (trend level, $p=0.09$); concentration, ns.
9
10
11
12
13

14 FIGURE 5. Overexpression of *fpn-1.1* in *pdr-1* mutants improves the DA-dependent basal slowing
15 response. Behavioral data are expressed as the change (Δ) in body bends per 20 seconds between treated
16 (5 mM $MnCl_2$) and untreated WT, *pdr-1* KO and *pdr-1* KO; *fpn-1.1* OVR animals placed on plates
17 without food vs. plates with food. Schematic shows the spectrum of change, with N2 wildtype animals
18 possessing a higher change in body bends (i.e., a fully intact DAergic system) to *cat-2* mutants possessing
19 a smaller, almost negligible change in body bends (i.e., an impaired DAergic system). *cat-2* KO animals
20 were used as a positive control. Statistical analysis by two-way ANOVA: interaction, ns (trend level,
21 $p=0.0872$); genotype, $p<0.0001$; concentration, ns. *** $p<0.001$ vs. untreated WT, * $p<0.05$ vs. *pdr-1* KO.
22
23
24
25
26
27
28
29
30
31
32
33
34
35
36
37
38
39
40
41
42
43
44
45
46
47
48
49
50
51
52
53
54
55
56
57
58
59
60